Infrasonic observations of open ocean swells in the Pacific: Deciphering the song of the sea

M. Willis,[1] M. Garcés, C. Hetzer, and S. Businger

Hawaii Institute of Geophysics and Planetology, School of Ocean and Earth Science and Technology, University of Hawaii at Manoa, Honolulu, Hawaii, USA

Received 4 June 2004; revised 21 July 2004; accepted 17 August 2004; published 7 October 2004.

[1] Microbaroms are infrasonic waves generated by nonlinear interactions of ocean surface waves traveling in nearly opposite directions with similar frequencies. Such interactions commonly occur between ocean waves with ~10 s periods, which are abundant in the open oceans and correspond to the observed 0.2 Hz infrasonic spectral peak. Microbarom observations from Hawai'i during 2002–2003 show a relationship with storm and ocean wave activity in the Pacific. Seasonal patterns of observed microbarom arrival azimuths are affected by the size and distribution of swells, by the dominant wind directions in the atmosphere, and by topographic shadowing. *INDEX TERMS:* 3339 Meteorology and Atmospheric Dynamics: Ocean/atmosphere interactions (0312, 4504); 3384 Meteorology and Atmospheric Dynamics: Waves and tides; 4231 Oceanography: General: Equatorial oceanography; 4263 Oceanography: General: Ocean prediction. **Citation:** Willis, M., M. Garcés, C. Hetzer, and S. Businger (2004), Infrasonic observations of open ocean swells in the Pacific: Deciphering the song of the sea, *Geophys. Res. Lett.*, *31*, L19303, doi:10.1029/2004GL020684.

1. Introduction

[2] Infrasound station IS59, located near Kailua-Kona, Hawaii, is part of the global infrasound network of the International Monitoring System (IMS) [*Vivas Veloso et al.*, 2002]. A large fraction of the ambient infrasonic field observed at IS59 is related to pervasive signals known as microbaroms. Microbaroms are observed as a continuous atmospheric pressure oscillation with most of its energy between 0.1 and 0.5 Hz (Figure 1). Microbaroms are detected at the IS59 arrays as coherent bursts with durations of minutes and have a RMS amplitude varying between ~10 mPa and ~100 mPa [*Willis*, 2004]. For infrasonic stations near the ocean, microbaroms comprise the low-wind noise floor. The microbarom peak is in the midst of the detection region for 1 kiloton nuclear explosion tests [*Stevens et al.*, 2002] and thus microbaroms can obscure an important signal of interest.

[3] Microbaroms were first reported by *Benioff and Gutenberg* [1939], although at the time of their studies there was no accepted hypothesis for microbaroms or their seismic counterparts, microseisms. *Longuet-Higgins* [1950] was the first to develop a mathematical theory for the excitation of microseisms by ocean waves. Studies by *Saxer* [1945, 1954], *Daniels* [1952, 1962], *Donn and Posmentier* [1967], *Donn and Naini* [1973] and *Rind* [1980] confirmed that microbarom and microseism sources are related to strong storms over the ocean and the resulting high seas. The accepted physical mechanism for microbarom generation is the nonlinear interactions of ocean surface waves traveling in nearly opposite directions with similar frequencies [e.g., *Arendt and Fritts*, 2000]. Microbaroms exhibit frequencies twice that of the individual ocean waves and amplitudes proportional to the product of the energy of the opposing wave trains [e.g., *Posmentier*, 1967; *Arendt and Fritts*, 2000].

2. Instrumentation and Data Analysis

[4] The IS59 infrasound array consists of four Chaparral-5 differential pressure microphones with a flat frequency response over the 0.05 to 8 Hz band. Three of the microphones are arranged as a triangle with a 2 km baseline, with the fourth sensor near the center of the triangle. Sensor data are recorded at 20 samples per second by 24-bit digitizers and sent in real time via radio telemetry to the Infrasound Laboratory at Keahole Point on the west coast of Hawaii. The IS59 station has very low ambient noise levels and is one of the most sensitive stations of the IMS because of its location in a dense tropical forest leeward of Hawaii's massive volcanoes. Porous hose filters are used for wind noise reduction.

[5] The Progressive Multi-Channel Correlation (PMCC) algorithm [*Cansi*, 1995; *Cansi and Klinger*, 1997] is the primary detection system used at IS59. A microbarom detection is only registered if the consistency is below 0.5 sec within the 0.1–0.5 Hz passband. The microbarom event processing scheme utilizes an analysis of overlapping windows of data (length – 90 sec, overlap – 70 sec). In essence, PMCC is used to detect coherent infrasonic energy across the array which allows the apparent horizontal phase speed, arrival azimuth, and amplitude of the detected arrivals to be extracted.

[6] Infrasonic power spectral densities are used to distinguish peaks in the microbarom frequency range. The power spectral densities were computed using the modified periodogram method [*Madisetti and Williams*, 1998] with a 102.4 s Hanning window (2^11 samples) and a 50% overlap. Power spectra include the combination of both coherent and incoherent microbarom contributions.

3. Microbarom Observations at IS59 During 2002–2003

[7] Strong microbarom signals tend to arrive from regions of marine storminess because they can produce

[1] Now at Surfline, Inc., 300 Pacific Coast Hwy. #310 Huntington Beach, CA 92648.

0094-8276/04/2004GL020684$05.00

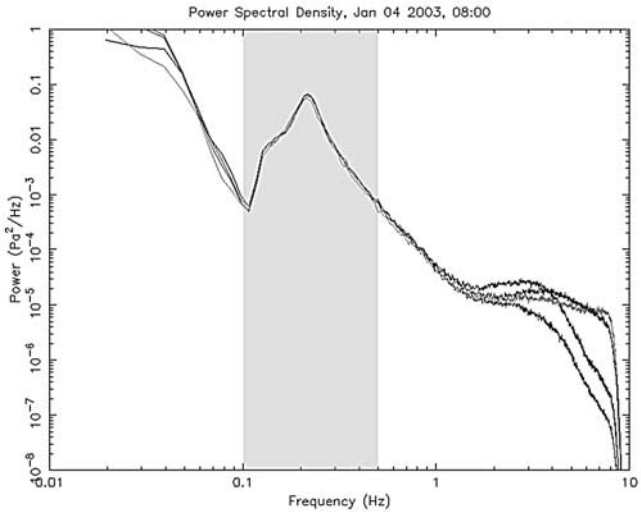

Figure 1. Infrasonic power spectral density observed at IS59 site on January 4, 2003 18Z (8am Local). The different lines represent power observed by the four components of the infrasonic array. Power spectral density (Pa^2/Hz) is on the vertical axis, acoustic frequency (Hz) is on the horizontal axis. The gray shaded region highlights the microbarom frequency range. The ~0.2 Hz peak, which theoretically corresponds to ocean waves of 10 sec, is observed throughout the year at IS59.

high amplitude ocean waves converging from opposite directions. By using ocean wave spectral output by the Wavewatch (WW3) model [*Tolman et al.*, 2002] in conjuction with the infrasonic source formulation of *Garcés et al.* [2003], *Willis* [2004] showed that strong microbarom source regions in the Pacific often occur in the wake regions of both mid-latitude and tropical cyclones, where swell spectra are confused with multidirectional components created ahead of and behind the surface low center (Figures 2 and 3). The wake region microbarom generation theory is discussed by *Ponomaryov et al.* [1998] and converging wave trains of opposite directions were also observed in the wake of Hurricane Bonnie [*Wright et al.*, 1998]. *Willis* [2004] also showed that strong signals can originate outside of storm wake regions (occasionally 1000–3000 km away from the wave producing winds), especially when multiple storms are present.

[8] Infrasonic power spectral densities at IS59 exhibit a quasi-permanent peak around ~0.2 Hz (Figure 1). This corresponds to the abundance of microbarom energy produced by opposing ocean waves containing periods of ~10 s. Occasionally, acoustic power at lower frequencies (~0.12–0.15 Hz) increases when strong storm systems are producing an abundance of interacting long period swell energy. This was shown by *Willis* [2004] from Jan. 4–6, 2003 in association with the strong storm shown in Figure 2.

[9] Coherent microbarom arrival azimuths and amplitudes at the IS59 site during 2002–2003 show an annual cycle (Figure 4). During the months from June through September microbarom arrivals generally come from east (55–130°) or south (160–220°) directions. The concentration of east arrivals is much stronger than the south arrivals during this time. Months October through March show an abundance of arrivals from 230–360° with a peak from northwesterly directions. Arrivals during April, May, late September and early October appear to arrive from a variety of different azimuths with no distinct peak noted. Annual arrivals correspond to dominant storm activity in the Pacific Basin but are also affected by topographic shadowing and zonal and meridional winds throughout the atmosphere. The effect of atmospheric winds on microbarom arrivals at IS59 are discussed in a companion paper (M. Garcés et al., On using ocean swells for continuous infrasonic measurements

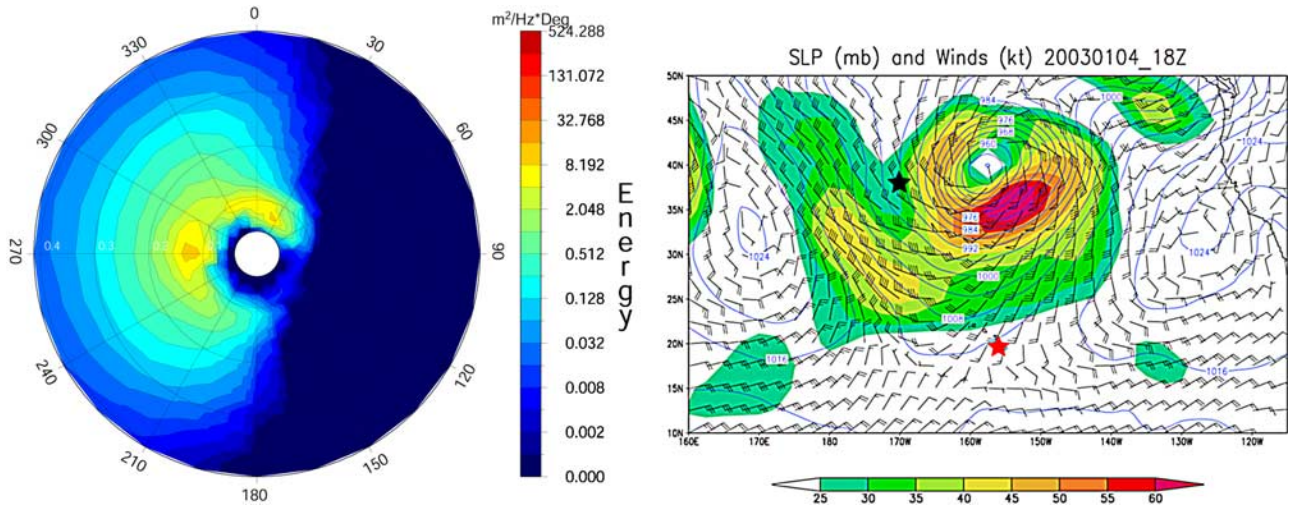

Figure 2. Polar plot (left) represents the directional ocean wave spectrum for a grid point (38.00N, 170.00W) at 18Z on Jan. 4, 2003 in the wake region of strong marine storm shown in adjacent plot of sea level pressure. Frequency (Hz) decreases towards the center, wave energy scale ($m^2/Hz*Deg$) on the right hand side. This ocean wave spectrum contains energy arriving from several directions and thus, microbarom generation is expected. The black star on the sea level pressure map (right) represents point of wave spectrum, the red star represents the location of IS59. Wave spectrum plotted using WW3 hindcast data. NCEP/NCAR Reanalysis data used to generate the surface weather plot.

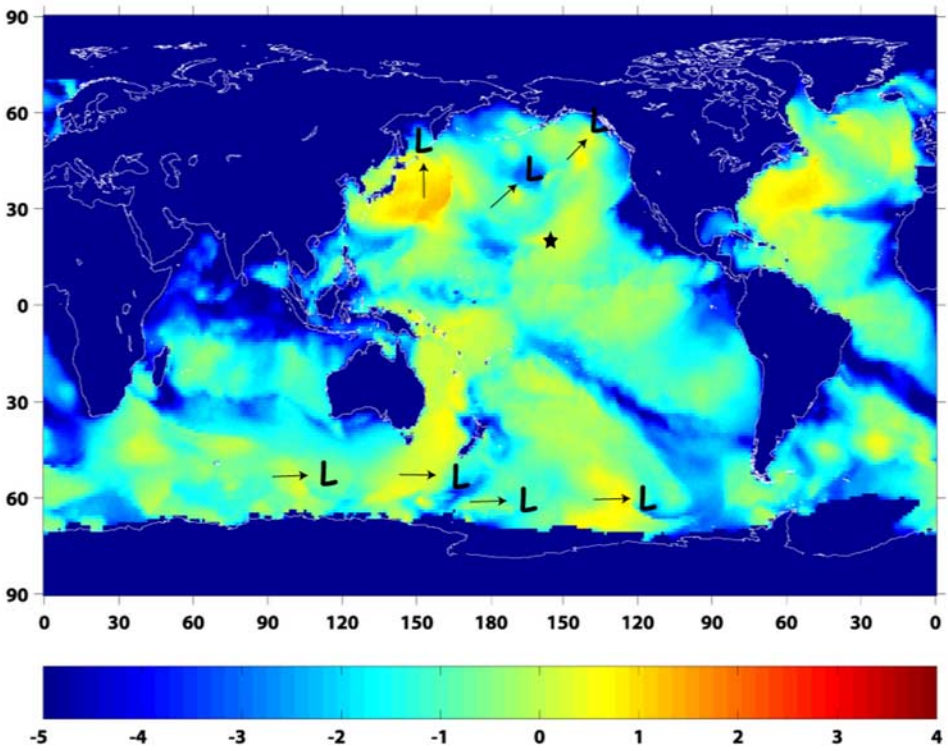

Figure 3. Base 10 logarithm of the magnitude of the acoustic source pressure spectrum (Pa * m^3) with frequency 0.197 Hz, corresponding to ocean waves interacting with periods of ~ 10 s (produced by equation 4 from spectral output given by WW3 as derived in *Willis*, 2004) on Jan. 4, 2003 18Z. The black star represents the location of IS59. Location of surface low-pressure centers in and near the Pacific are indicated with "L" and storm propagation directions are indicated with arrows. Each storm exhibits a modeled peak in acoustic source pressure in its wake region, though high source values are also present at great distances from marine storms. This shows how common it is to have opposing swell trains, and thus microbarom production, anytime and anywhere in the Pacific basin.

of winds and temperature in the lower, middle, and upper atmosphere, submitted to *Geophysical Research Letters*, 2004, hereinafter referred to as Garcés et al., submitted manuscript, 2004).

[10] A total of 21459 coherent microbarom arrivals reached IS59 in 2003. 9334 of these arrivals (43%), the vast majority, came from 270–315°. The second highest 45 degree directional bin, 225–270°, contained 4211 (19.6%) microbarom arrivals during 2003. 2606 arrivals (12%) came from 45–90°, 1605 (7.5%) from 315–360°, 1599 (7.5%) from 180–225°, 1168 (5.4%) from 0–45°, 549 from 90–135°, while only 377 arrivals came from azimuths 135–180°.

[11] During the first quarter of 2003 (containing months December 2002, January and February 2003), 98% of the microbarom arrivals came from azimuths 225–360°. The second quarter of 2003 (March, April, May) shows a similar directional dependence with 81% of the arrivals coming from 225–360°. However, stronger signatures from 0–90° (13%) and 180–225° (4%) were evident in quarter 2 than in quarter 1.

[12] A very different pattern of microbarom arrival azimuth was observed during the boreal summer months. 70% of the arrivals during June, July, and August came from 0–135° while 26% came from 135–225°. Arrivals at IS59 during the fall months of quarter 4 (September, October, November) show a very similar pattern to the springtime quarter 2 arrivals – with 72% coming from 225–360°, 13% from 0–90°, and 10% from 180–225°.

4. Conclusions and Discussion

[13] Microbaroms are generated wherever ocean surface waves traveling in nearly opposite directions with similar frequencies meet. This situation commonly occurs with

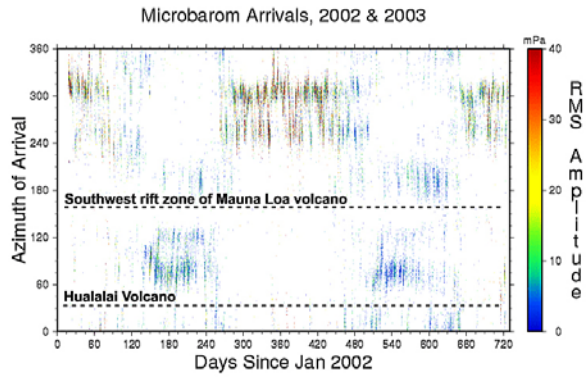

Figure 4. Infrasonic wave arrival azimuth and amplitude of coherent microbarom arrivals at IS59 during 2003. Arrival azimuth at the array is measured clockwise from north (0° to 360°).

ocean waves of periods near 10 s, particularly in storm wake regions. Thus, a quasi-permanent infrasonic spectral peak of 0.2 Hz is observed at IS59 as well as most infrasound stations in the world. In the case of an eastward moving middle latitude storm (Figure 2), the south side of the storm will contain the strongest fetch lengths, durations, and intensities and thus higher wave heights and periods can be expected on the south of the center. It is rare for an eastward moving storm to produce long wave periods of 13 seconds or more on the north side of the center unless the storm is a slow mover, large in diameter, and quite strong [*Morris and Nelson*, 1977]. Furthermore, since long period swells exhibit higher group velocities than short period swells, unless a storm is very large, symmetrical, and fast moving, the long period energy created ahead of a low center will often be dispersed and not have time to interact with any longer period energy that may be created behind the low center. This is especially true when the storm is moving slower than the group velocities of the long period ocean waves it produces. For example, ocean waves with periods of 13 s travel with a group velocity of nearly 20 kt. In order for 13 s swell energy of equal but opposite directions to interact (created ahead of and behind the low center), the storm system must be moving $\geq$20 kt. Steep, short period swells (<8 seconds) often dissipate within a few wavelengths due to whitecapping and angular spreading effects. This can prevent opposing wave trains of short periods from interacting. On the other hand, opposing wave trains of medium periods (8–12 seconds) are very likely in wake of both middle latitude and tropical cyclones, which supports the commonly observed infrasonic peak at 0.2 Hz. If there are long period swells created on the north side of the center, the amplitudes are normally small and thus the resulting infrasonic wave will also have small amplitude. Similarly, dissipating shorter period swells that may interact will also produce smaller amplitude infrasonic waves. This also helps explain the common infrasonic spectral peak at 0.2 Hz.

[14] Coherent microbarom arrivals at IS59 during 2003 suggest a relationship between microbarom arrival azimuth and dominant storm activity in the Pacific Basin (Figure 4). Northern hemisphere winter arrivals at IS59 come from west and northwest directions, while summer arrivals come primarily from east and south azimuths. Arrivals during the shoulder seasons are more evenly distributed around the compass. Microbaroms observed at IS59 come primarily from regions where storm and wave activity are the strongest throughout the year, and the seasonal trend roughly coincides with the stratospheric wind patterns (see Garcés et al., submitted manuscript, 2004). The seasonal pattern of coherent microbarom amplitudes may be due to the closer distance of the source to the receiver during winter. Propagation path effects may also play a role, and will be addressed in a separate study. Figure 4 also shows evidence for acoustic shadowing by adjacent Mauna Loa and Hualalai volcanoes, which shelter the array from the trade winds. Reflections from the coastline may also contribute to a portion of the arrivals from 45 to 95° at IS59, especially during summer months when trade winds are present 80–90% of the time near the Hawaiian Islands [*Sanderson*, 1993].

[15] Although in general the continuous microbarom noise is uncorrelated at IS59, distinct coherent microbarom packets can be detected in the Hawaii array. When designing an array it may be useful to retain the coherence of microbaroms, as then it may be possible to remove this contribution from a signal of interest. There is also potential for using microbaroms to monitor ocean wave activity, since microbaroms contain information about the wave periods and amplitudes of the generating open ocean waves.

[16] **Acknowledgments.** This work has been funded by Defense Threat Reduction Agency contracts DTRA01-00-C-0106 and DTRA01-01-C-0077. Paul Wittmann (FNMOC) provided the guidance in getting WW3 operational for this research.

References

Arendt, S., and D. Fritts (2000), Acoustic radiation by ocean surface waves, *J. Fluid Mech.*, *415*, 1–21.

Benioff, H., and B. Gutenberg (1939), Waves and currents recorded by electromagnetic barographs, *Bull. Am. Meteorol. Soc.*, *20*, 421.

Cansi, Y. (1995), An automatic seismic event processing for detection and location: The P. M. C. C. method, *Geophys. Res. Lett.*, *22*, 1021–1024.

Cansi, Y., and Y. Klinger (1997), An automated data processing method for mini-arrays, *Newslett. Eur. Mediter. Seismol. Cent.*, *11*, 2–4.

Daniels, F. B. (1952), Acoustical energy generated by the ocean waves, *J. Acoust. Soc. Am.*, *24*, 83.

Daniels, F. B. (1962), Generation of infrasound by ocean waves, *J. Acoust. Soc. Am.*, *34*, 352–353.

Donn, W. L., and B. Naini (1973), Sea wave origin of microbaroms and microseisms, *J. Geophys. Res.*, *78*, 4482–4488.

Donn, W. L., and E. S. Posmentier (1967), Infrasonic waves from the marine storm of April 7, 1966, *J. Geophys. Res.*, *72*, 2053–2061.

Garcés, M., C. Hetzer, M. Willis, and S. Businger (2003), Integration of infrasonic models with ocean wave spectra and atmospheric specifications to produce global estimates of microbarom signal levels, paper presented at 25th Seismic Research Review, Nucl. Security Admin. and Air Force Res. Lab., Tucson, Ariz.

Madisetti, V. K., and D. B. Williams (1998), *The Digital Processing Handbook*, CRC Press, Boca Raton, Fla.

Morris, V., and J. Nelson (1977), *The Weather Surfer*, 103 pp., Grossmont Press, San Diego, Calif.

Longuet-Higgins, M. S. (1950), A theory of the origin of microseisms, *Philos. Trans. R. Soc. London, Ser. A*, *243*, 1–35.

Ponomaryov, E. A., A. G. Sorokin, and V. N. Tabulevich (1998), Microseisms and infrasound: A kind of remote sensing, *Phys. Earth Planet. Inter.*, *108*, 339–346.

Posmentier, E. (1967), A theory of microbaroms, *Geophys. J. R. Astron. Soc.*, *13*, 487–501.

Rind, D. (1980), Microseisms at Palisades 3: Microseisms and microbaroms, *J. Geophys. Res.*, *85*, 4854–4862.

Sanderson, M. (Ed.) (1993), *Prevailing Trade Winds*, pp. 12–36, Univ. of Hawaii Press, Honolulu.

Saxer, L. (1945), Electrische Messung kleiner atmospharischer Druckshwankingen, *Helv. Phys. Acta*, *18*, 527.

Saxer, L. (1954), Über Entstehung und Ausbreitung quasiperiodischer Luftdruckschwankungen, *Arch. Meteorol. Geophys. Bioklimatol., Ser. A*, *6*, 451–457.

Stevens, J., I. Divnov, D. Adams, J. Murphy, and V. Bourchik (2002), Constraints on infrasound scaling and attenuation relations from Soviet explosion data, *Pure Appl. Geophys.*, *159*, 1045–1062.

Tolman, H., B. Balasubramaniyan, L. Burroughs, D. Chalikov, Y. Chao, H. Chen, and V. Gerald (2002), Development and implementation of ocean surface wave models at NCEP, *Weather Forecasting*, *17*, 311–333.

Vivas Veloso, J., et al. (2002), Status of the IMS infrasound network, paper presented at the Infrasound Technology Workshop, R. Neth. Meteorol. Inst., De Bilt, Netherlands, 28–31 Oct.

Willis, M. (2004), Observations and source modeling of microbaroms in the Pacific, M.S. thesis, Dept. of Meteorology, University of Hawaii at Manoa, 77 pp.

Wright, C. W., E. J. Walsh, D. Vandemark, W. B. Krabill, A. W. Garcia, S. H. Houston, M. D. Powell, P. G. Black, and F. D. Marks (1998), Hurricane directional wave spectrum variation in the open ocean, *J. Phys. Oceanogr.*, *31*, 2472–2488.

S. Businger, M. Garcés, C. Hetzer, and M. Willis, HIGP, SOEST, University of Hawaii at Manoa, UHM 73-4460, Queen Kaahumanu Hwy #119, Kailua-Kona, HI 96740-2638, USA. (milton@isla.hawaii.edu)